ARTICLE

BIOTECHNOLOGY and BIOENGINEERING

A New Method for Generating High Purity Motoneurons From Mouse Embryonic Stem Cells

Dylan A. McCreedy,[1] Chelsea R. Brown,[1] Jessica C. Butts,[1] Hao Xu,[1] James E. Huettner,[2] Shelly E. Sakiyama-Elbert[1]

[1]Department of Biomedical Engineering, Washington University in St. Louis, St. Louis, Missouri 63130; telephone: 314-935-7556; fax: 314-935-7448; e-mail: sakiyama@wustl.edu

[2]Department of Cell Biology and Physiology, Washington University School of Medicine, St. Louis, Missouri

ABSTRACT: A common problem with using embryonic stem (ES) cells as a source for analysis of gene expression, drug toxicity, or functional characterization studies is the heterogeneity that results from many differentiation protocols. The ability to generate large numbers of high purity differentiated cells from pluripotent stem cells could greatly enhance their utility for in vitro characterization studies and transplantation in pre-clinical injury models. Population heterogeneity is particularly troublesome for post-mitotic neurons, including motoneurons, because they do not proliferate and are quickly diluted in culture by proliferative phenotypes, such as glia. Studies of motoneuron biology and disease, in particular amyotrophic lateral sclerosis, can benefit from high purity motoneuron cultures. In this study, we engineered a transgenic-ES cell line where highly conserved enhancer elements for the motoneuron transcription factor Hb9 were used to drive puromycin *N*-acetyltransferase expression in ES cell-derived motoneurons. Antibiotic selection with puromycin was then used to obtain high purity motoneuron cultures following differentiation of mouse ES cells. Purity was maintained during maturation allowing the production of consistent, uniform populations of cholinergic ES cell-derived motoneurons. Appropriate functional properties of purified motoneurons were verified by acetylcholinesterase activity and electrophysiology. Antibiotic selection, therefore, can provide an inexpensive alternative to current methods for isolating ES cell-derived motoneurons at high purity that does not require specialized laboratory equipment and provides a unique platform for studies in motoneuron development and degeneration.

Biotechnol. Bioeng. 2014;111: 2041–2055.

KEYWORDS: puromycin selection; electrophysiology; transcription factor; neural differentiation

Introduction

The ability to culture neurons in vitro has many advantages including applications in toxicology screening, developmental studies, and cell replacement strategies. Embryonic stem (ES) cells hold great potential as an expandable cell source that can be differentiated into specific neuronal sub-types by recapitulating developmental signals. The signaling events necessary for differentiation of ES cells into mid-brain dopaminergic neurons (Lee et al., 2000), cortical pyramidal neurons (Gaspard et al., 2009), cerebellar neurons (Salero and Hatten, 2007), dorsal interneurons (Murashov et al., 2005), and spinal motoneurons (Wichterle et al., 2002) have been previously described. ES cell-derived neurons have been shown to maintain neuronal sub-type-specific properties and have the potential to integrate when transplanted into appropriate regions of the central nervous system (Espuny-Camacho et al., 2013; Kim et al., 2002; Wichterle et al., 2009). Furthermore, transplanted mouse ES cell-derived motoneurons have been shown to restore partial motor function following selective ablation of host spinal motoneurons in rats (Deshpande et al., 2006).

The directed differentiation of ES cells into spinal motoneurons can be achieved by exposure of embryoid bodies (EBs) to retinoic acid (RA) and sonic hedgehog (Shh) (Wichterle and Peljto, 2008). RA serves as a caudalizing signal to generate spinal progenitor cells, while Shh acts as a ventralizing agent to induce differentiation into progenitor motoneurons (pMNs) expressing the basic helix-loop-helix

Disclosure statement: The authors state that they have no conflict of interest to declare.

Authors contributions: Dylan A. McCreedy: conception and design, collection and assembly of data, data analysis and interpretation, manuscript writing, final approval of manuscript. Chelsea R. Brown: collection and assembly of data, data analysis and interpretation, manuscript writing, final approval of manuscript. Jessica C. Butts: collection and assembly of data, data analysis and interpretation, manuscript writing, final approval of manuscript. Hao Xu: collection and assembly of data, manuscript writing, final approval of manuscript. James E. Huettner: Conception and design, collection and assembly of data, data analysis and interpretation, provision of study material, manuscript writing, final approval of manuscript. Shelly E. Sakiyama-Elbert: conception and design, financial support, administrative support, data interpretation, provision of study material, manuscript writing, final approval of manuscript.

Correspondence to: S.E. Sakiyama-Elbert

Contract grant sponsor: NIH
Contract grant number: R01 NS051454
Contract grant sponsor: NSF Graduate Research Fellowship
Received 19 December 2013; Revision received 27 March 2014; Accepted 31 March 2014
Accepted manuscript online 19 May 2014;
Article first published online 4 June 2014 in Wiley Online Library (http://onlinelibrary.wiley.com/doi/10.1002/bit.25260/abstract).
DOI 10.1002/bit.25260

transcription factor Olig2. Spinal motoneurons differentiate from pMNs by expressing the homeobox domain transcription factor Hb9 and down-regulating Olig2 (Arber et al., 1999). In addition to motoneurons, pMNs also give rise to oligodendrocytes and astrocytes in vitro (Xian and Gottlieb, 2004). The efficiency of differentiation into pMNs can be enhanced by use of small molecule agonists of the Shh pathway, resulting in up to 50% of the total cell population expressing Hb9 (Amoroso et al., 2013; Li et al., 2008). Postmitotic motoneurons, however, are diluted as a percentage of the total cell population by the continuing proliferation of glia during extended culture. High purity mature motoneuron cultures may be desired to control neuron–glia interactions and evaluate motoneuron viability in cellular models of amyotrophic lateral sclerosis (ALS) and spinal muscular atrophy.

Several methods have been developed to purify motoneurons from mixed cell cultures. Isolation of MNs from mouse (Gingras et al., 2007), rat (Schnaar and Schaffner, 1981), and chick (Schnaar and Schaffner, 1981) fetal spinal cord has been demonstrated using density gradient centrifugation to separate large motoneurons based on cell density. While initially successful, this technique cannot guarantee removal of glia. When applied to human and monkey ES cell-derived motoneurons, gradient centrifugation provided only partial enrichment of motoneurons (Wada et al., 2009). Purity following extended culture of enriched human ES cell-derived motoneurons, however, was not demonstrated. Alternatively, the Hb9 promoter has been used to drive enhanced green fluorescent protein (eGFP) expression for visual identification and fluorescence-activated cell sorting (FACS) of ES cell-derived motoneurons (Singh et al., 2005). FACS, however, is time intensive and requires a central facility with expensive equipment, and it also has the potential to contaminate cell cultures. Other methods have been utilized to purify motoneurons, including panning for the low-affinity nerve growth factor receptor (p75), but these approaches may limited by technical difficulty and yield (Camu and Henderson, 1992; Veyrat-Durebex et al., 2013).

The development of a low-cost technique for producing high purity ES cell-derived motoneurons can provide a powerful tool to enable studies of neurodegenerative diseases and development. In this study, we obtained high purity cultures by antibiotic selection of ES cell-derived motoneurons. Mouse ES cells were transfected with a selection vector containing two highly conserved enhancers of the Hb9 gene driving the puromycin resistance enzyme, puromycin *N*-acetyltransferase (PAC). Following differentiation of ES cells into motoneurons, addition of puromycin to the culture media killed cells not expressing Hb9. Motoneuron purity was demonstrated immediately following puromycin selection and was maintained through maturation cultures. High purity motoneurons matured into functional cholinergic neurons as determined by expression of choline acetyltransferase (ChAT), acetylcholinesterase (AChE) activity, and electrophysiology. This technique provides an inexpensive and scalable method for obtaining high purity mature motoneuron cultures.

Materials and Methods

Embryonic Stem Cell Culture

Transgenic and RW4 (American Type Culture Collection, Manassas, VA) mouse ES cells were cultured on gelatin-coated T-25 flasks in complete media consisting of Dulbecco's Modified Eagle Medium (DMEM; Life Technologies, Carlsbad, CA) containing 10% newborn calf serum (Life Technologies), 10% fetal bovine serum (Life Technologies), 10 μM thymidine (Sigma, St. Louis, MO), and 30 μM of each of the following nucleosides (Sigma): adenosine, cytosine, guanosine, and uridine. For routine culture, ES cells were passaged every 2 days. Briefly, ES cells were washed with DMEM containing 25 mM HEPES (Life Technologies) and dissociated with 0.25% trypsin-EDTA (Life Technologies) for 5 min. Trypsin was quenched with fresh complete media and cells were transferred to a new gelatin-coated flask at a 1:5 ratio in fresh complete media containing 1,000 U/mL of leukemia inhibitory factor (LIF; Millipore, Bellerica, MA) and 100 μM β-mercaptoethanol (BME; Life Technologies).

Hb9-Puro Selection Vector

Hb9 enhancers A and B followed by the minimal β-globin promoter were PCR amplified from the CSH2IV vector (kind gift from Patrick Blanner). The resulting PCR product was cut and ligated into a vector containing the puromycin resistance cassette (kind gift from David Gottlieb). The resistance cassette also contained the gene for a neomycin resistance enzyme, neomycin phosphotransferase, driven by the ubiquitously expressed phosphoglycerate kinase (PGK) promoter for identification of integration events. The PGK promoter and the neomycin phosphotransferase gene were flanked by loxP sites to facilitate removal following integration of the Hb9-Puro vector. Ligated vector was amplified in DH5α *Escherichia coli* and isolated using a mini-prep kit (Qiagen, Hilden, DE).

Electroporation and Clonal Analysis

RW4 ES cells were used to make a transgenic-ES cell line. Approximately 10×10^6 ES cells were resuspended in electroporation buffer with 10 μg Sal1 linearized Hb9-Puro selection vector. Cells were electroporated at 0.23 kV and 960 μF in a 0.4-cm cuvette (Bio-Rad, Hercules, CA) and plated on 100-mm gelatin-coated petri dishes in complete media with 1,000 U/mL of LIF, 100 μM of BME, and 40 μg/mL of geneticin (Life Technologies). Media was replaced every 2 days. After 9 days, single colonies were picked and plated in individual wells of a gelatin-coated 48-well plate containing complete media with 1,000 U/mL of LIF and 100 μM of BME. Clones were screened for puromycin resistance at the ES cell state and resistant clones were discarded. A total of 24 transgenic clones were screened for puromycin resistance in motoneurons following motoneuron differentiation (see "Motoneuron Differentiation" and "Motoneuron Selection" sections in methods).

Transgenic clones with puromycin-resistant motoneurons were analyzed for PAC copy number by qRT-PCR (Mancini et al., 2011). PAC and glyceraldehyde 3-phosphate dehydrogenase (GAPDH) sequences were amplified from genomic DNA using TaqMan assays (Life Technologies) and TaqMan Genotyping Master Mix (Life Technologies) per manufacturer's instructions. A total of 10 ng of genomic DNA per reaction was used. Quantitative delta-Ct values for PAC were obtained using GAPDH as an endogenous control. Copy number standard curves were made by diluting Hb9-Puro plasmid DNA in RW4 genomic DNA. The calculated copy number of each clone was normalized to the calculated copy number for the P-Olig2 ES cell line, which has been previously demonstrated to contain a single PAC insertion (McCreedy et al., 2012).

Cre Excision

The pTurboCre plasmid (kind gift from David Gottlieb) was used to remove the PGK promoter and neomycin phosphotransferase gene from transgenic-ES cells derived from a single transgenic clone. Approximately 3 ng of plasmid was incubated in Opti-MEM media (Life Technologies) and Lipofectamine 2000 (Life Technologies). Half of the culture media was replaced with Opti-MEM media containing pTurboCre plasmid and Lipofectamine 2000 for 4 h. Media was then replaced with complete media containing LIF and BME and cells were allowed to recover overnight. The following day, ES cell cultures were dissociated and plated at 6×10^3 cells/cm^2 in individual wells of a gelatin-coated 6-well plate in complete media with 1,000 U/mL of LIF, 100 μM of BME, and 40 μg/mL of geneticin. After 9 days, single colonies were picked and plated in individual wells of a gelatin-coated 48-well plate containing complete media with LIF and BME. Clones were screened for sensitivity to neomycin by exposure to 40 μg/mL of geneticin for 5 days, and those that were not sensitive were discarded. A single transgenic clone was used to derive the transgenic-ES cell line used for the remainder of the study.

Motoneuron Differentiation

Transgenic-ES cells were differentiated into motoneurons using a $2^-/4^+$ RA and smoothened agonist (SAG, Millipore) induction protocol as previously described (McCreedy et al., 2012). Approximately 1×10^6 ES cells were cultured in suspension on agar-coated 100-mm petri dishes in modified DFK5 media consisting of DMEM/F12 base media (Life Technologies) containing 5% knockout serum replacement (Life Technologies), 1× insulin transferrin selenium (Life Technologies), 50 μM of nonessential amino acids (Life Technologies), 100 μM of BME, 5 μM of thymidine, and 15 μM of the following nucleosides: adenosine, cytosine, guanosine, and uridine. During this process, ES cells aggregate into multi-cellular EBs. After the first 2 days (2^-), the EBs were moved to a 15 mL of conical and allowed to settle for 5 min. The media was aspirated and replaced with 10 mL of fresh DFK5 containing 2 μM of RA and 600 nM of SAG. In differentiated control cultures, the Shh antagonist cyclopamine (Cyc, 1 μM; Sigma) was used instead of SAG. EBs were then cultured for an additional 4 days (4^+), and media was replaced every 2 days.

Motoneuron Selection

Transgenic-ES cells differentiated using the $2^-/4^+$ RA and SAG induction were dissociated in 0.25% Trypsin-EDTA for 15 min and quenched with complete media. Dissociated cells were counted and centrifuged at 240*g* for 5 min. Cells were resuspended in DFK5 media containing 5 ng/mL of glial-derived neurotrophic factor (GDNF; Peprotech, Rocky Hill, NJ), 5 ng/mL of brain-derived neurotrophic factor (BDNF; Peprotech), 5 ng/mL of neurotrophin-3 (NT-3; Peprotech), 4 μg/mL of puromycin in water (Sigma) and plated at 1.5×10^5 cells/cm^2 in individual wells of a laminin-coated 6-well plate for 24 h. In parallel control cultures not receiving puromycin, cells were resuspended in DFK5 media with the growth factor cocktail and plated at 7.5×10^4 cells/cm^2 in individual wells of a laminin-coated 6-well plate for 24 h. Following selection, cells were fixed for immunofluorescence or media was replaced with modified DFKNB media consisting of DFK5 and Neural basal (NB) media (Life Technologies) mixed at a 1:1 ratio and supplemented with B27, 5 ng/mL of GDNF, 5 ng/mL of BDNF, and 5 ng/mL of NT-3. Cells were cultured in DFKNB media for up to 8 additional days.

Polymerase Chain Reaction

Cell lysates were collected using an RNeasy kit (Qiagen) from ES cells, ES cells differentiated with the $2^-/4^+$ RA and SAG or the $2^-/4^+$ RA and Cyc induction protocol. Fifty nanograms of mRNA from each sample was amplified using a One-Step PCR Kit (Qiagen). Primers for Hb9 were as follows: 5′-GGCCATAGGATGGGATTGTA-3′ (forward) and 5′-CGGCGCTTCCTACTCATAC-3′ (reverse).

Cell Viability Assay

To determine cell viability after puromycin selection, ES cells were differentiated using the $2^-/4^+$ RA and SAG or the control $2^-/4^+$ RA and Cyc induction protocol. Differentiated cells and undifferentiated ES cells were dissociated and plated in individual wells of laminin-coated 6-well plate in DFK5 media with 4 μg/mL of puromycin at a density of 6×10^4 cells/cm^2 and 4×10^4 cells/cm^2, respectively. Cells were selected with puromycin for 24 h. Control cultures not receiving puromycin were run in parallel. Following puromycin selection, media was replaced with fresh DFK5 containing calcein-AM (Life Technologies) for 30 min. Fluorescent images were captured using a MICROfire (Olympus, Center Valley, PA) camera attached to an Olympus IX70 inverted microscope.

Transcription Factor Analysis

Due to the short temporal expression of the Olig2 and Hb9 transcription factors, ES cells were differentiated using a modified $2^-/4^+$ RA and SAG exposure protocol, where EBs were dissociated at $2^-/3^+$ and plated in individual wells of a laminin-coated 6-well plates in fresh DFK5 media containing 2 μM of RA, 600 nM of SAG, and 2 μg/mL of puromycin for 20 h prior to fixation for immunofluorescence. Control cultures without puromycin for the 20-h selection period were run in parallel. Culture were fixed following selection and analyzed by immunofluorescence (see "Immunofluorescence and Cell Counting" section).

Immunofluorescence and Cell Counting

Cells were fixed in 4% (w/v) paraformaldehyde (Sigma) in phosphate-buffered saline (PBS) for 15 min at room temperature. Fixed cultures were washed once with PBS, and the cells were permeabilized with 0.1% triton-X in PBS for 15 min. Cultures were then blocked for 1 h at 4°C with 5% normal goat serum (NGS; Sigma) in PBS. Primary antibodies were added to blocked cultures overnight at 4°C at the following dilutions in 2% NGS in PBS: neurofilament (NF, 1:50, Iowa Developmental Studies Hybridoma Bank [DSHB], Iowa City, IA), Olig2 (1:400, Millipore), MNR2/Hb9 (1:20, DSHB), β-tubulin class III (β-TubIII, 1:400, Millipore), ChAT (1:500, Millipore), FoxP1 (1:500, AbCam, Cambridge, MA), Lhx3 (1:2,000, DSHB), Ki67 (1:250, AbCam), or glial fibrillary acidic protein (GFAP, 1:100, ImmunoStar, Hudson, WI). Primary antibodies were bound with the appropriate AlexaFluor conjugated goat antibodies (Life Technologies) at a 1:200 dilution in 2% NGS in PBS for 4 h. All wells were counterstained with the Hoechst (1:1,000; Life Technologies) to label cell nuclei. Following immunofluorescence, phase contrast, and fluorescent images were captured. Live cells were identified by phase contrast and Hoechst staining. Cells with apparent processes and round nuclei were included in the cell counting experiments. Cells with fragmented nuclei demonstrating evidence of cell death were not included in total cell counts. Cell counting was performed using ImageJ (NIH, Bethesda, MD) software. Approximately 500 cells were counted per replicate.

AChE Staining

A modified Karnovsky stain was used to assess AChE activity in motoneurons. Cells were washed with PBS and fixed in 4% paraformaldehyde in PBS for 30 min. The wells were washed with water and incubated in AChE staining solution consisting of 65 mM of phosphate buffer (pH = 6.0; Sigma), 10 mg/mL of gelatin (Sigma), 5 mM of sodium citrate (Sigma), 3 mM of copper sulfate (Sigma), 0.5 mM of potassium ferricyanide (Sigma), 0.2 mM of ethropropazine (Sigma), and 4 mM of acetylthiocholine (Sigma) for 7 days. Wells were rinse five times with water. Water was removed and Prolong Gold mounting solution containing DAPI (Life Technologies) was added to each well. A coverslip was carefully placed over the well and mounting solution was allowed to harden overnight at room temperature. Brightfield images and fluorescent images were taken the following day.

Electrophysiology

Cultures were bath perfused with Tyrode's solution (in mM, all from Sigma): 150 NaCl, 4 KCl, 2 $MgCl_2$, 2 $CaCl_2$, 10 glucose, 10 HEPES, pH adjusted to 7.4 with NaOH. Whole-cell electrodes pulled from borosilicate glass capillaries had an open tip resistance of 2–5 MOhm when filled with one of the following internal solutions (in mM, all from Sigma): (1) 140 K-glucuronate, 10 NaCl, 5 $MgCl_2$, 0.2 EGTA, 5 Na-ATP, 1 Na-GTP, 10 HEPES, pH adjusted to 7.4 with KOH; (2) 140 Cs-glucuronate, 5 CsCl, 5 $MgCl_2$, 10 EGTA, 5 Na-ATP, 1 Na-GTP, 10 HEPES, pH adjusted to 7.4 with CsOH; or (3) 120 tetraethylammonium (TEA) chloride, 5 $MgCl_2$, 5 Na-ATP, 1 Na-GTP, 10 EGTA, 10 HEPES, pH adjusted to 7.4 with TEA-hydroxide. Current and voltage were recorded with an Axopatch 200A amplifier, filtered at 1 kHz, digitized at 10 kHz and analyzed off-line with Clampfit software (pClamp 9.2, Molecular Devices, Sunnyvale, PA). Voltage-gated channel antagonists tetrodotoxin (TTX, Sigma) and 4-aminopyridine (4-AP, Sigma) were dissolved in Tyrode's solution and delivered under gravity flow from a local perfusion pipette (Kim et al., 2009). Ligand-gated channel agonists were dissolved in 160 NaCl, 10 HEPES, 2 $CaCl_2$ at 100 μM and also applied by local perfusion.

Statistical Analysis

Unless otherwise noted all measured parameters are reported as mean ± SEM. Statistical significance was determined by Scheffe's post hoc test for analysis of variance (ANOVA) using Statistica software (version 5.5; StatSoft, Tulsa, OK). Significance was assigned for *P*-values less than 0.05.

Results

Hb9 Enhancers Drive Puromycin Resistance Following Differentiation of Embryonic Stem Cells into Motoneurons

Differentiation of ES cells using RA and Shh gives rise to multiple cell types (Fig. 1). To isolate motoneurons from the diverse cell population, we developed a new selection vector (Hb9-Puro) containing previously identified enhancer elements of the motoneuron transcription factor, Hb9, driving the puromycin resistance enzyme, PAC (Fig. 2A; Nakano et al., 2005). The Hb9-Puro selection vector was electroporated into ES cells, and the resulting cultures were screened for neomycin resistance to ensure genomic incorporation of the vector. Twenty-four transgenic clones were isolated and 12 demonstrated puromycin resistance in motoneurons. The total transgenic copy number varied from approximately 0.25–9 insertions (Table SI). A single clone with approximately one copy of the PAC gene as

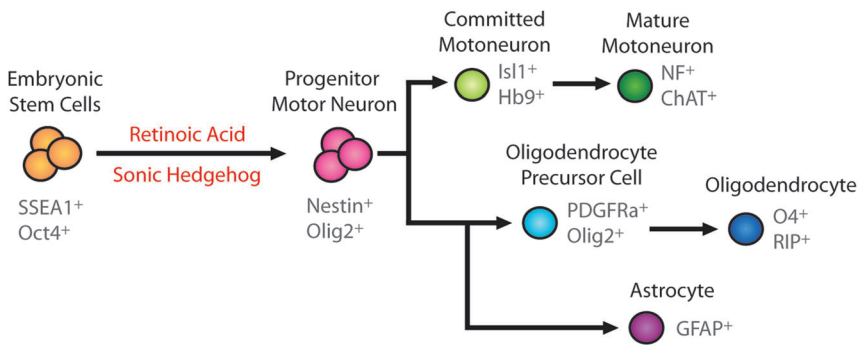

Figure 1. Motoneuron differentiation of ES cells following RA and Shh induction. Following the $2^-/4^+$ induction protocol, ES cells differentiate into tri-potent pMNs. The resulting pMNs can differentiate into motoneurons, astrocytes, or oligodendrocytes. Markers for each cell type are shown in gray.

demonstrated by qRT-PCR was then treated with cre recombinase to remove the neomycin selection cassette that is flanked by loxP sites. The last step was performed to eliminate potential off-target *cis*-regulation of the neighboring PAC gene by the PGK promoter as previously demonstrated (Anderson et al., 2007).

The resulting transgenic-ES cell line was used for all subsequent analysis in this study. Transgenic-ES cell cultures were aggregated for 2 days (2^-) to form EBs as part of a $2^-/4^+$ induction protocol. EBs were exposed to RA and SAG, for 4 days (4^+) to induce differentiation into motoneurons. Undifferentiated ES cells and ES cells differentiated with RA and the Shh antagonist, Cyc were used as controls. Cells from each group were lysed and presence of Hb9 mRNA was assessed by RT-PCR. In cultures receiving RA and SAG, Hb9 mRNA was detected by PCR (Fig. 2B). No Hb9 mRNA was observed in either control group.

To determine if Hb9 expression led to expression of PAC, cultures differentiated with RA and SAG were dissociated following the $2^-/4^+$ induction protocol and plated on laminin-coated wells with puromycin (4 μg/mL) in the media for 24 h. Parallel cultures not receiving puromycin, as well as undifferentiated ES cells and ES cells differentiated with RA and Cyc, were used as controls. In the absence of puromycin, all cultures contained viable cells as evidenced by calcien AM fluorescence (Fig. 2C). With puromycin, undifferentiated ES cells and ES cells differentiated with RA and Cyc did not survive. Viable cells, however, were present following puromycin selection for ES cells differentiated with RA and SAG. Surviving cells displayed phase bright cell bodies and long neurites, morphology consistent with neuronal differentiation.

Surviving Cells Label for Immature Motoneuron Markers Immediately Following Puromycin Selection

To determine if Hb9 enhancer-driven puromycin resistance was specific to motoneurons, we investigated the expression

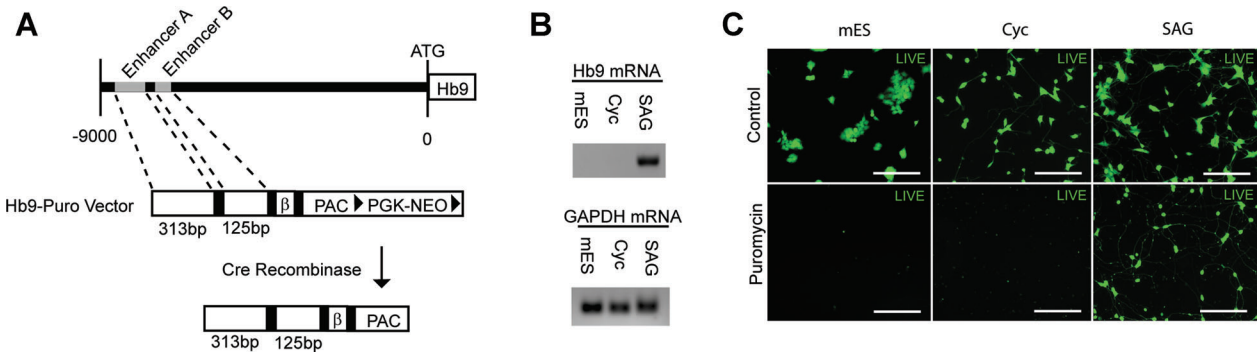

Figure 2. Hb9-Puro selection vector and puromycin resistance. **A**: Schematic showing location of Hb9 enhancers A and B upstream of Hb9 gene. Enhancers A and B were used in conjunction with the minimal β-globin promoter (β) to drive PAC expression. Neomycin phosphotransferase expression was driven by the ubiquitously expressed PGK promoter for identification of cells with incorporated vector. Cre recombinase was used to remove the PGK promoter and neomycin phosphotransferase gene following incorporation into ES cells. **B**: Hb9 mRNA expression in ES cells (ES), ES cells differentiated with RA and Cyc (Cyc), and ES cells differentiated with RA and SAG (SAG). **C**: Live cell assay in ES cells, ES cells differentiated with RA and Cyc (Cyc), and ES cells differentiated with RA and SAG (SAG) following puromycin selection. Control cultures were run in parallel without puromycin.

of Olig2 and Hb9, two transcription factors associated with motoneuron development and differentiation. Due to the short temporal expression of Olig2 and Hb9, a modified $2^-/4^+$ induction and selection protocol was used. ES cells were aggregated for 2 days into EBs and exposed to RA and SAG for 3 days ($2^-/3^+$). EBs were then dissociated and plated on laminin-coated plates with puromycin, RA, and SAG for 20 h (Fig. 3A). In parallel cultures not receiving puromycin, $32.3 \pm 1.7\%$ of cells stained positive for the pMN transcription factor Olig2 and $46.3 \pm 1.0\%$ of cells stained positive for motoneuron transcription factor Hb9 (Fig. 3B and C). When puromycin was added during the 20-h selection period, no cells labeled for Olig2 ($n = 3$, $P < 0.001$) while $98.3 \pm 0.10\%$ of cells were positive for Hb9 ($n = 3$, $P < 0.001$). Remaining viable cells had a consistent neuronal morphology.

To increase the number of surviving cells for analysis of the neuron-specific marker β-tubIII, ES cells were aggregated for 2 days then exposed to RA and SAG for 4 days ($2^-/4^+$), at which time Hb9 is highly expressed (McCreedy et al., 2012). EBs were then dissociated and plated on laminin-coated wells for 24 h with puromycin (Fig. 3D). In parallel control cultures without puromycin, many cells were observed with glial morphology and did not express β-tubIII (Fig. 3E). Approximately $59.7 \pm 2.79\%$ of cells stained positive for β-tubIII at the end of the 24-h period in control cultures without puromycin selection. In cultures receiving puromycin for 24 h, cells with glial morphology were not observed. The percentage of cells expressing β-tubIII significantly increased to $98.90 \pm 0.20\%$ following puromycin selection ($n = 3$, $P < 0.001$, Fig. 3F). Selected motoneurons also labeled

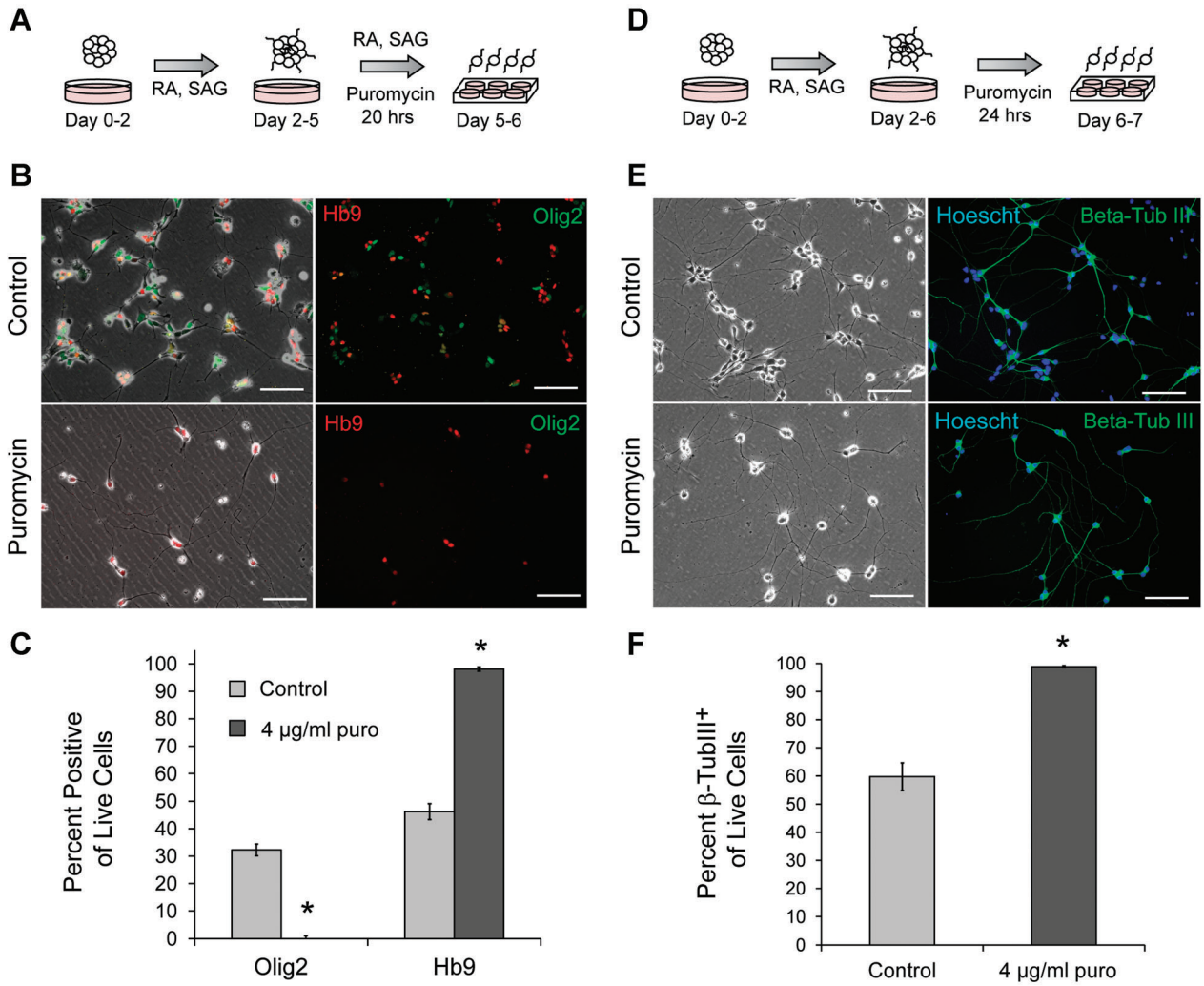

Figure 3. Puromycin selection of transgenic-ES cells. **A**: Schematic of modified $2^-/4^+$ induction protocol including the 20-h puromycin selection. Puromycin was added for 20 h between Days 5 and 6. **B**: Immunofluorescence analysis of Olig2 and Hb9 transcription factors following puromycin selection in culture not receiving puromycin (control) and selected with 4 μg/mL of puromycin (puromycin). **C**: Counting analysis of control and puromycin-selected cultures. **D**: Schematic of $2^-/4^+$ induction protocol followed by a 24-h puromycin selection. Puromycin was added for 24 h between Days 6 and 7. **E**: Immunofluorescence analysis of β-tubulin class III (β-tubIII) following puromycin selection. **F**: Counting analysis of control and puromycin-selected cultures. $^*P < 0.001$ for each marker compared to control group. Scale bars = 100 μM.

with Lhx3 and FoxP1, demonstrating median motor column identity and lateral motor column identity, respectively (Fig. 4).

High Purity Motoneurons Achieve Functional Maturation

To determine if immature motoneurons could achieve functional maturation following puromycin selection, ES cells were differentiated using the $2^-/4^+$ RA and Shh induction protocol and selected with puromycin for 24 h on laminin-coated wells. Cultures without puromycin were run in parallel. Following selection, cultures were switched to DFKNB media without puromycin for 5 days prior to fixation (Fig. 5A). In selected cultures, cells displayed large neuronal cell bodies and long branching neurites, morphology typical of mature motoneurons. When labeled for the mature neuronal marker NF, $99.40 \pm 0.61\%$ of cells were NF-positive in selected cultures while only $5.42 \pm 1.24\%$ of cells expressed NF in control cultures not receiving puromycin ($n = 3$, $P < 0.001$, Fig. 5B). Large NF^+ neurites were observed extending between cell bodies of neurons in both cultures (Fig. 5C).

Mature motoneurons contain AChE and ChAT enzymatic activity. Poor staining with ChAT antibodies by immunofluorescence in vitro has been previously reported (Bohl et al., 2008). Karnovsky staining has been utilized to differentially label motor nerves from sensory nerves via AChE activity (Kanaya et al., 1991). Similar assays have been used to label motoneurons in culture where antibodies for ChAT were inconclusive. We employed a modified version of the Karnovsky stain to assess AChE activity in fixed cultures (Bohl et al., 2008; Gruber and Zenker, 1973; Kanaya et al., 1991). In this process, the enzymatic activity of AChE facilitates a chemical reaction resulting in Hatchett's Brown precipitate. In control cultures, precipitate was observed in cells with neuronal morphology (Fig. 5C). Labeled cells accounted for $30.60 \pm 1.67\%$ of cells in the absence of puromycin. Significantly more cells, $99.30 \pm 0.43\%$ ($n = 3$, $P < 0.001$), contained precipitate in selected cultures and all cells displayed neuronal morphology (Fig. 5C). Neurons in the selected cultures displayed remarkably larger somas, typical of mature motoneurons, compared with control cultures.

Cultures were also stained for ChAT to confirm the cholinergic identity of motoneurons (Fig. 5D and E). Bright fluorescence was observed in control and selected cultures. In control cultures, dim non-specific staining was observed in cells with glial morphology preventing accurate assessment of cell purity. Almost all cells labeled with the ChAT antibody in cultures receiving puromycin.

Selected Cultures Are Post-Mitotic and Maintain Purity After Extended Maturation

Neural differentiation of ES cells results in many glial subtypes that rapidly proliferate and reduce neuronal purity. Astrocytes are one of the first mature glial cells to differentiate from glial progenitors. To evaluate the presence of astrocytes, cultures were allowed to mature for 7 days following puromycin selection (Fig. 6A). Cultures were then fixed and labeled for GFAP. In control cultures not receiving puromycin, $GFAP^+$ astrocytes were frequently observed

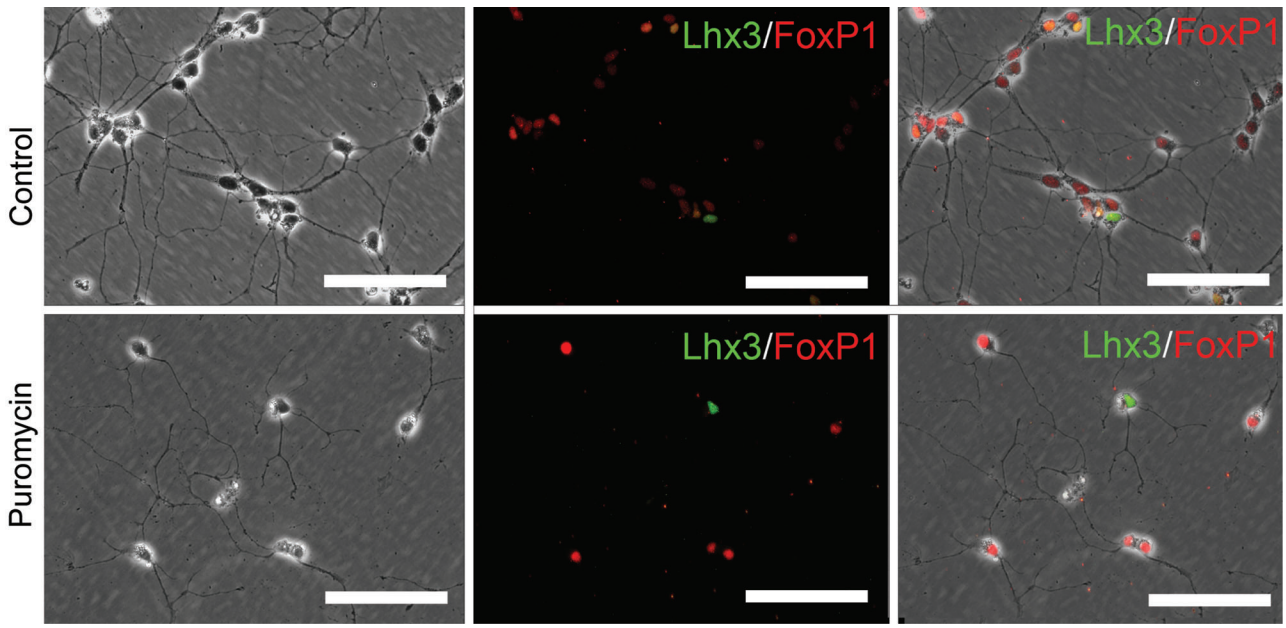

Figure 4. Immunofluorescence staining of motoneurons sub-type markers. Following the $2^-/4^+$ induction protocol and subsequent 24-h puromycin selection, cells were labeled with FoxP1 (red) and Lhx3 (green) to label distinct motor column identities in control (top) cultures and selected (bottom) cultures.

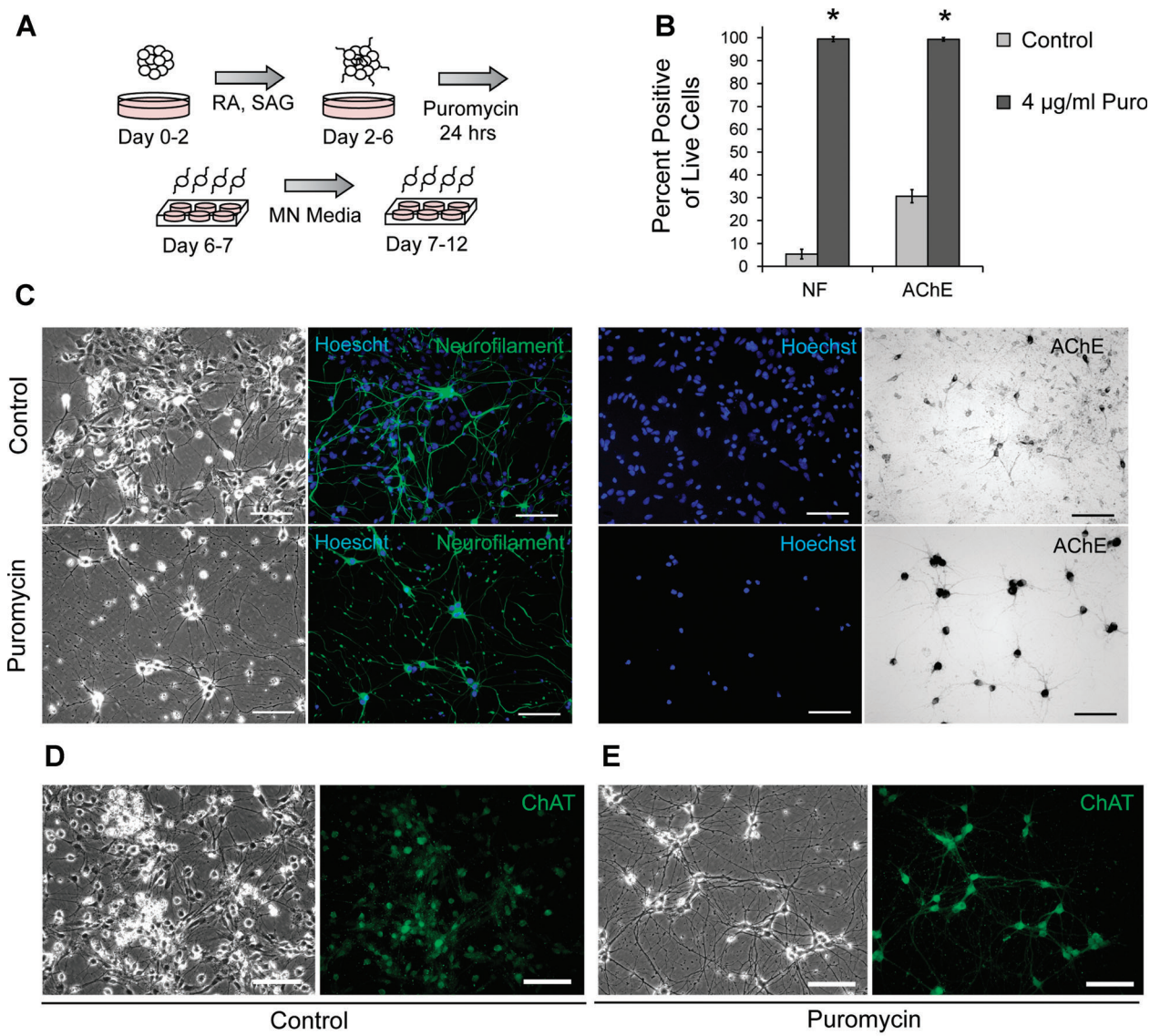

Figure 5. Maturation of puromycin-selected motoneurons. **A**: Schematic of $2^-/4^+$ induction protocol followed by a 24-h puromycin selection and 5-day extended culture. Puromycin was added for 24 h between Days 6 and 7. Media was replaced with DFKNB media immediately following selection and cultures were continued for an additional 5 days. **B**: Counting analysis of control and puromycin-selected cultures for neurofilament (NF) marker and acetylcholinesterase (AChE) assay. **C**: Immunofluorescence analysis of NF and AChE following 5-day extended culture. **D** and **E**: Immunofluorescence staining of choline acetyltransferase (ChAT) in control (**D**) and selected (**E**) cultures. $^*P < 0.001$ for each marker compared to control group. Scale bars = 100 μM.

(Fig. 6B). No GFAP labeling, however, was observed in any cultures receiving puromycin for 24 h. Cells in selected cultures maintained neuronal morphology with large cells bodies and branched neurites.

Motoneurons are post-mitotic and will not proliferate like their glial counterparts. To assess proliferation, ES cells were differentiated using the $2^-/4^+$ RA and SAG protocol and plated on laminin-coated-wells for 24 h with puromycin in the culture media. Control cultures without puromycin were run in parallel. The total number of cell nuclei was assessed immediately following selection, at 3 days, and at 5 days post-selection. Control cultures contained $29.6 \pm 6.9 \times 10^3$ cells/cm^2, while selected cultures contained $9.3 \pm 1.2 \times 10^3$ cells/cm^2 post-selection. The number of cells in control cultures increased to 82.7×10^3 cells/cm^2 and 147.8×10^3 cells/cm^2 at 3 and 5 days after the selection period, respectively. Normalized to the first day following selection, there was approximately a 2.8- and 5-fold increase in cells for control cultures not receiving puromycin (Fig. 6C). A decrease in cell number was observed in selected cultures to 6.4×10^3 cells/cm^2 (0.68-fold change) and 5.8×10^3 cells/cm^2 (0.62-fold change) at 3 and 5 days post-selection suggesting that proliferating cells were absent. No Ki67$^+$ cells were observed in selected cultures, whereas

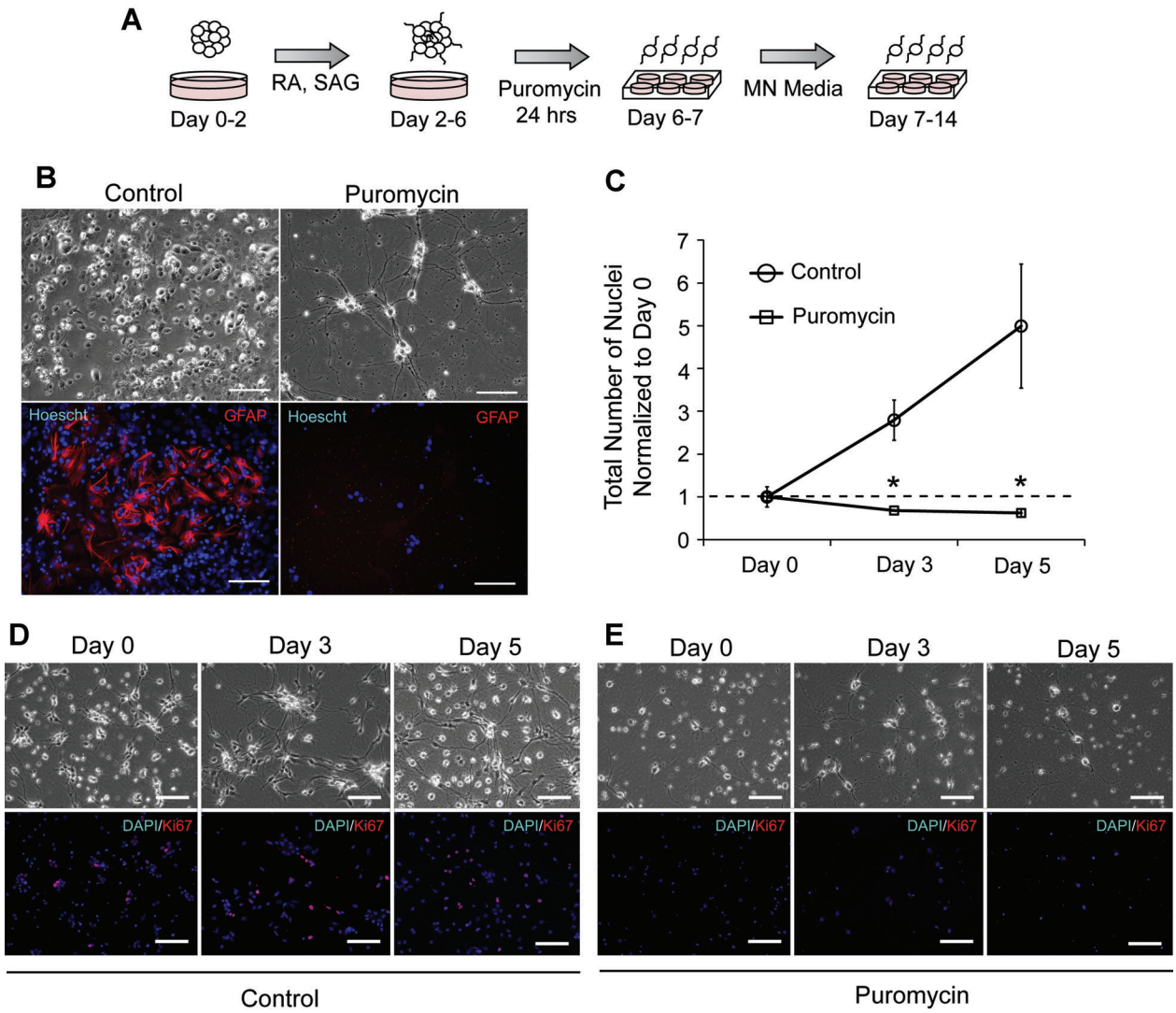

Figure 6. Glial differentiation and proliferation following puromycin selection. **A**: Schematic of $2^-/4^+$ induction protocol followed by a 24-h puromycin selection and 7-day extended culture. Puromycin was added for 24 h between Days 6 and 7. Media was replaced with maturation media immediately following selection and cultures were continued for an additional 7 days. **B**: Immunofluorescence analysis of glial fibrillary acidic protein (GFAP, astrocytes) expression in culture 7 days post-selection. **C**: Total nuclei counts immediately post-selection (Day 0) continuing 3 and 5 days post-selection. Total nuclei number was normalized to Day 0. **D**: Immunofluorescence analysis of the proliferation marker Ki67 in control and **E**: selected cultures at 0, 3, and 5 Days following the $2^-/4^+$ induction protocol. $^*P < 0.05$ for selected group compared with control group. Scale bars = 100 μM.

control cultures contained many cells labeling with Ki67 (Fig. 6D and E). The fold changes in control and selected cultures were significantly different at 3 and 5 days post-selection ($n = 3$, $P < 0.05$).

Selected Cultures Maintain Mature Electrophysiological Properties

To determine whether our puromycin selection process had any detrimental effects on the ability of ES cell-derived motoneurons to undergo functional differentiation, we performed whole-cell current- and voltage-clamp recordings between 0 and 7 days after puromycin selection (Days 0–7). When stimulated by depolarizing current injection, cells recorded under current clamp at Days 2–7 fired action potentials (Fig. 7A) with a mean threshold of -34.1 ± 1.5 mV ($n = 19$). More than half of the cells maintained a negative resting membrane potential (< -50 mV) without the need for DC hyperpolarization. The average resting membrane potential (V_{rest}) in these cells was -60.4 ± 1.2 mV ($n = 10$). For long duration current pulses (800 ms) roughly one-third of the cells only fired single action potentials, another third fired multiple spikes, but with low frequency (10–15 Hz) and substantial adaptation in spike amplitude, while the remaining cells fired repeatedly at 20–25 Hz and with much less spike amplitude adaptation (Figs. 7A and 8).

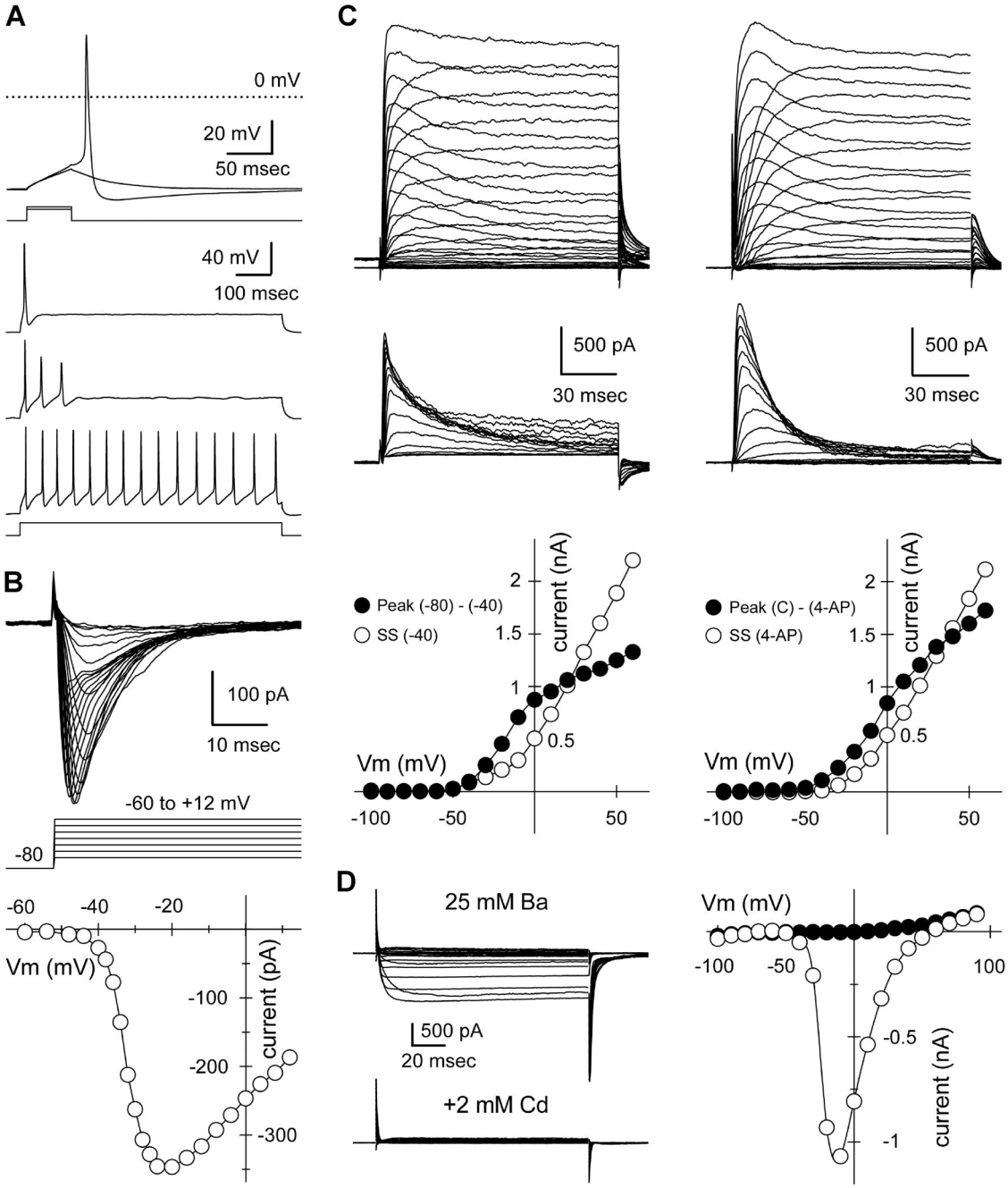

Figure 7. Action potentials and voltage-gated whole-cell currents. **A**: Sub- and supra-threshold voltage responses recorded under current clamp with 50 ms square pulse current injections (30 and 34 pA); examples of action potential firing patterns in three different cells stimulated with 800 ms square pulse current injections (K-glucuronate internal solution, Day 7 after selection). **B**: Voltage-gated sodium channel currents evoked by steps from −60 to +12 mV from a holding potential of −80 mV; (below) Current–voltage relation for peak inward currents (TEA-chloride internal solution, Day 5 after selection). **C**: Transient and sustained voltage-gated potassium channel currents evoked by steps from −100 to +60 mV from holding potentials of −80 and/or −40 mV in Tyrodes external solution containing 0.5 μM TTX. Left: Transient currents revealed by subtracting non-inactivating currents evoked while holding at −40 mV from the combined currents evoked while holding at −80 mV; Day 4 after selection. Right: Currents evoked in the absence and presence of 4-aminopyridine (5 mM) from a holding potential of −80, Day 6 after selection. Transient currents revealed by subtracting non-inactivating currents evoked in the presence of 4-AP from the combined currents evoked in control external solution. Current–voltage relations for peak outward transient (filled circles) and steady-state (open circles) currents (K-glucuronate internal solution). **D**: Current mediated by voltage-gated calcium channels evoked by steps from −100 to +90 mV from a holding potential of −80 mV. Top left: Currents in TEA-chloride with 25 mM $BaCl_2$ as the charge carrier; bottom left: with addition of the calcium channel antagonist $CdCl_2$ (2 mM). Right: Current–voltage relation for peak inward currents in the absence (open circles) and presence (filled circles) of cadmium. TEA-chloride internal solution, Day 8 after selection.

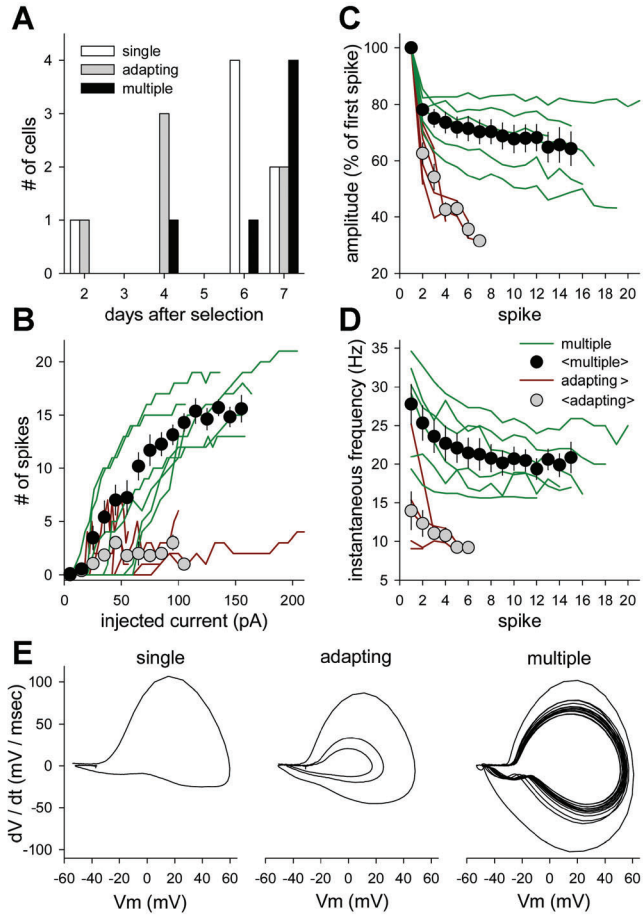

Figure 8. Action potential properties in selected motoneurons. **A**: Histogram of firing pattern in 19 cells as a function of days after selection (two cells, Day 2; four cells, Day 4; five cells, Day 6; eight cells, Day 7). Cells spiking was classified as single, adapting or multiple for 800 ms square pulse stimulation as shown in Figure 7A. **B**: Number of action potentials increased more steeply with injected current for cells in the multiple spike category. **C**: Peak amplitude declined more gradually with spike number in the multiple spike category. **D**: Both adapting and multiple spike cells displayed spike frequency adaptation, but adapting cells fired at lower frequency (10–15 Hz) on average than multiple spiking cells (20–25 Hz). **E**: Phase plots (dV/dt vs. V_m) for 800 ms square pulse stimulation voltage responses of the single spike, adapting and multiple spike cells shown in Figure 7A. Firing threshold was determined from the phase plot inflection point of the first spike.

Under voltage-clamp, steps from a holding potential of −80 mV to more depolarized test potentials evoked fast transient inward currents (Fig. 7B) that were blocked by the sodium channel antagonist TTX (Fig. 7C); and, more slowly activating, and partially inactivating, outward currents (Fig. 7C) that were largely eliminated when potassium in the internal solution was substituted with cesium (Cs) or TEA. In addition, the transient component of outward current was selectively inhibited by holding at −40 mV or by extracellular exposure to 5 mM 4-AP (Fig. 7C). Lower doses of 4-AP (500 μM), which selectively block transient outward current in some cell types (Bean, 2007), had minimal effect on currents recorded in our puromycin-selected motoneurons ($n = 6$). In addition to voltage-gated sodium and potassium currents, the selected motoneurons also displayed cadmium-sensitive currents mediated by voltage-gated calcium channels (Fig. 7D), which were recorded using 5 or 25 mM barium as the charge carrier and with both internal and external monovalent cations largely replaced by TEA. Table SII summarizes parameters in the puromycin-selected motoneurons for activation and steady-state inactivation of voltage-gated sodium and transient potassium currents, as well as activation parameters for sustained potassium and calcium currents (Fig. 9).

To test for expression of functional neurotransmitter receptors we exposed cells to selective agonists for AMPA/kainate, NMDA, glycine, and GABA receptors, all of which

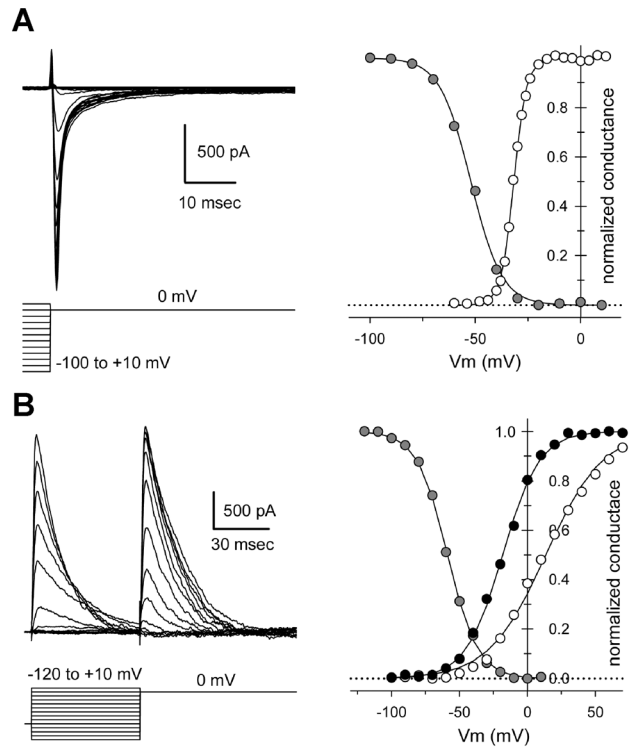

Figure 9. Steady-state inactivation of voltage-gated sodium and transient potassium channel currents. **A**: Whole-cell currents (control − TTX) evoked by a step to 0 mV following 60 ms pre-pulses from −100 to +10 mV (Cs-glucuronate internal solution, Day 5 after selection). Right: Current–voltage relations for sodium current steady-state inactivation (gray circles) for this cell and for activation (open circles) for the cell in Figure 7B. Smooth curves are best-fit Boltzmann functions for activation $G = 1/(1 + \exp[-(V - V_h)/k])$, where V is the step potential in mV, $V_h = -31.7$ mV is the voltage for half-maximal activation and $k = 3.1$ is the slope factor in mV; and, for inactivation $G = 1/(1 + \exp[(V - V_h)/k])$, where $V_h = -52.1$ mV and $k = 7.4$ mV. **B**: Whole-cell currents (control − 4-AP) evoked by a step to 0 mV following 60 ms pre-pulses from −120 to +10 mV (K-glucuronate internal solution, Day 7 after selection). Right: Current–voltage relations for steady-state inactivation (gray circles) for this cell and for activation of steady state (open circles) and peak transient (black circles) outward current for the cell in Figure 7C. Smooth curves are best-fit Boltzmann functions for inactivation $G = 1/(1 + \exp[(V - V_h)/k])$, where V is the step potential in mV, $V_h = -58.8$ mV is the voltage for half-maximal inactivation and $k = 11.1$ is the slope factor in mV; and, for activation $G = 1/(1 + \exp[-(V - V_h)/k])$, $V_h = -18.3$ mV, $k = 13.4$ mV for transient current and $V_h = 13.5$ mV, $k = 20.7$ mV for steady-state current.

activated inward current when applied at 100 μM while holding cells at a fixed potential of −80 mV (Fig. 10A). To evaluate the permeation properties of channels that underlie these responses, we applied the agonists while ramping the membrane potential from −100 to +100 mV (Fig. 10B). As expected for inhibitory chloride-selective channels the currents evoked by glycine and GABA reversed polarity near −50 mV, which is close to the calculated equilibrium potential for chloride during these recordings (−54 mV). In contrast, the currents evoked by excitatory glutamate receptor agonists kainate and NMDA reversed polarity near 0 mV, consistent with activation of non-selective cation channels (Traynelis et al., 2010). Figure 10C plots the mean amplitude of agonist-activated currents recorded 0, 2, 4, and 6 days after puromycin selection showing that responses increased as differentiation proceeded. Over this same time period whole-cell capacitance, which is proportional to surface area, increased from 22.6 ± 1.5 pF at Day 0 ($n = 11$) to a plateau of 54.1 ± 2.7 pF between Days 5 and 8 ($n = 52$). Although the currents evoked by NMDA were small at all time points and required a low concentration (1 μM) of the co-agonist glycine (Bean, 2007), the difference in reversal potential between currents evoked by NMDA (9.1 ± 6.6 mV, $n = 6$) and glycine (−53.2 ± 1.2 mV, $n = 10$) confirm that the current evoked by 100 μM NMDA with 1 μM glycine is mediated by NMDA receptors and not by weak activation of glycine receptors. In addition, the large increase in current variance apparent in Figure 10A during exposure to NMDA is consistent with the high unitary conductance of NMDA receptor channels (Traynelis et al., 2010).

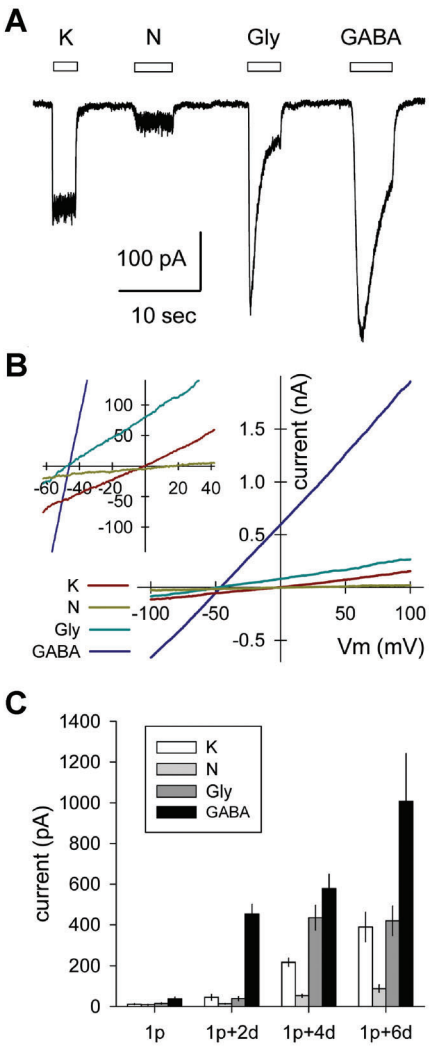

Figure 10. Whole-cell currents activated by excitatory and inhibitory agonists. **A**: Open boxes indicate periods of exposure to 100 μM kainate (K), 100 μM NMDA (N, plus 1 μM glycine), 100 μM glycine (Gly), and 100 μM GABA (K-glucuronate internal solution, 4 days after selection). **B**: Current–voltage relations for agonist-activated whole-cell currents as membrane potential was ramped from −100 to +100 mV at 1.2 mV/ms. Lines plot the current recorded during agonist exposure minus current in control extracellular solution. Note that in this cell the currents evoked by inhibitory agonists Gly (teal) and GABA (blue) reverse polarity near −47 mV, consistent with chloride-selective channels, whereas the excitatory agonists K (red) and N (gold) reverse near 0 mV, as expected for cation selective channels (Cs-glucuronate internal solution, Day 4 after selection). On average, the reversal potentials were 0.9 ± 2.4 mV for kainate ($n = 7$), 9.1 ± 6.6 mV for NMDA ($n = 6$), −53.2 ± 1.2 mV for glycine ($n = 10$) and −51.4 ± 1.5 mV ($n = 8$) for GABA. **C**: Agonist-activated currents increase with time after puromycin selection ($n = 7$ to 19 cells per time point).

Taken together, our physiological data are largely in agreement with previous work on motoneurons derived from in vitro differentiation of mouse (Miles et al., 2004) and human (Takazawa et al., 2012) ES cells, and with studies of primary motoneurons in dissociated culture (Carrascal et al., 2005). Mouse (Miles et al., 2004) and human (Takazawa et al., 2012) ES-derived motoneurons, as well as primary motoneurons in culture (Carrascal et al., 2005) develop the ability to fire multiple spikes during periods of prolonged depolarization, but also exhibit adaptation in both spike frequency and amplitude (see Fig. 10). In addition, analysis of mouse ES-derived neurons expressing GFP under control of the Hb9 promoter (Miles et al., 2004) demonstrated acquisition of both transient and sustained voltage-gated potassium currents, as well as voltage-gated sodium and calcium currents and transmitter-gated currents activated by GABA, glycine and by glutamate (see Table SIII).

Discussion

ES cells provide an important tool that allows the study of a variety of cell types in culture that may be difficult to isolate from primary tissue. Obtaining high purity ES cell-derived populations, however, can be difficult due to the heterogeneity in cultures obtained following current differentiation protocols. The MYH6 promoter has been previously used to drive puromycin resistance in ES cell-derived cardiomyocytes leading to significant enrichment (91.5 ± 4.3% purity) following selection (Anderson et al., 2007). We have recently used homologous recombination at the Olig2 locus to confer puromycin resistance and isolate pMNs from differentiated ES cell cultures (McCreedy et al., 2012). While promising, these studies have failed to produce near pure cultures (>99%) of a single cell type. The identification of two unique enhancers of the motoneurons associated gene Hb9, or

MNX1 in the human genome, has allowed for specific labeling of motoneurons within the mouse spinal cord (Nakano et al., 2005). Furthermore, a 3.6 kb region including these enhancers has been used to drive GFP expression in ES cell-derived motoneurons for FACS (Singh et al., 2005). To determine if these enhancers could drive puromycin resistance in motoneurons, we created a selection vector with the Hb9 enhancers driving expression of the puromycin resistance enzyme, PAC.

Transgenic mouse ES cells, generated by electroporation of a linearized Hb9-Puro selection vector, maintained normal motoneuron differentiation with Hb9 mRNA only detected following the $2^{-}/4^{+}$ RA and Shh induction protocol. The Shh antagonist, Cyc inhibited any detectable expression of Hb9 by PCR. Viable cells were only observed following puromycin selection in cultures differentiated with RA and the Shh signaling agonist, SAG. These data indicate that expression of PAC correlates with Hb9 expression as expected. Furthermore, the two Hb9 enhancers in tandem were sufficient, along with the minimal β-globin promoter, to provide puromycin resistance.

In motoneurons development, Olig2 expression precedes the expression of Hb9. Following commitment to the motoneurons fate, Hb9 is up-regulated as Olig2 is down-regulated. In selected cultures, no Olig2 expression was observed. The absence of $Olig2^{+}$ cells demonstrates the appropriate temporal regulation of the Hb9-Puro selection vector. Selected cultures stained positive for other appropriate markers for immature neurons including β-tubIII, FoxP1, and Lhx3. These results demonstrate that expression of PAC by the Hb9-Puro selection vector is temporally and spatially restricted to cells committed to the motoneuron fate and can be used to generate high purity (>99%) cultures.

In studies focused on isolating motoneurons from heterogeneous cell populations, the extended culture of motoneurons beyond 2 days while maintaining purity has yet to be demonstrated (Gingras et al., 2007; Wada et al., 2009). Furthermore, the maturation of motoneurons in the absence of astrocyte feeder layers is limited. In the current study, greater than 99% of the cells in selected cultures stained positive for the neuronal marker NF at the end of the extended cultures (up to 5 days). Selected motoneurons were able to mature while neuronal purity was maintained at 5 days post-selection. High purity cultures also labeled with the AChE assay, demonstrating appropriate enzymatic activity. AChE is found in any neuronal sub-type capable of receiving cholinergic input and is not specific to motoneurons. ChAT provides a more specific marker for motoneurons. While ChAT immunolabeling was observed counting was not possible due to non-specific staining in control cultures. The poor performance of ChAT antibodies for in vitro labeling of motoneurons has been previously reported (Bohl et al., 2008). In selected cultures, large cells bodies with prominent neurite branching were observed almost exclusively. Labeled neurons in control cultures were less uniform and appeared to mature at a slower rate, possibly due to factors secreted by undesired cell types or neuron–glia interactions. To our knowledge, this is the first study to demonstrated high purity mature motoneurons cultures without the need of astrocytes feeder layers.

The functional properties of ES cell-derived motoneurons cultured on mouse myotubes have been previously investigated (Miles et al., 2004). To determine if isolated motoneurons maintain similar electrophysiological properties, we performed whole-cell patch-clamp recordings during maturation of selected motoneurons. High purity motoneurons displayed transient sodium and potassium currents, as well as sustained potassium and calcium currents. Both inward sodium and outward transient potassium currents could by inactivated by pre-pulse steps. Increasing currents were observed during maturation of motoneurons in response to agonists for ligand-gate ion channels. Furthermore, selected motoneurons were able to fire multiple action potentials. These results demonstrate that isolated motoneurons maintain functional properties. Integration of the Hb9-Puro vector into the mouse genome and subsequent puromycin selection did not appear to hinder appropriate development of selected motoneurons.

The technique utilized in this study may be advantageous for other systems where yield of the desired cell type is low including human ES cell-derived motoneurons, induced

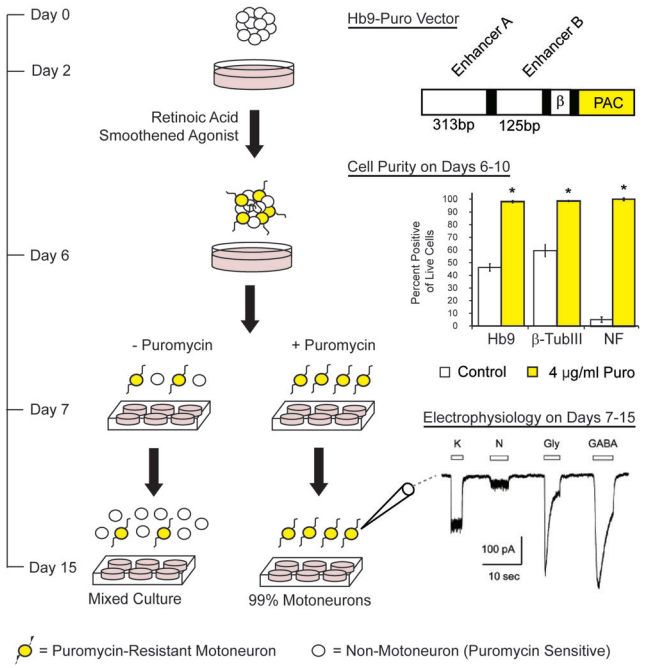

Figure 11. Overview of the experimental process and data collected. ES cells were aggregated into EBs (Days 0–2) and then exposed to retinoic acid (RA) and smoothened agonist (SAG) for 4 days (Days 2–6). EBs were dissociated and plated in media containing puromycin or in control media not containing puromycin for 24 h. Cells were allowed to mature for an additional 8 days following puromycin removal. Cell purity was assessed at Days 6 (Hb9), 7 (β-TubIII), and 10 (NF). Electrophysiology was performed on Days 7–15. * $P < 0.001$ for each marker compared with control group. NF, neurofilament; β-TubIII, β-tubulin class III; PAC, puromycin *N*-acetyltransferase; Gly, glycine; N, NMDA; K, kainite.

pluripotent stem cell-derived motoneurons, and direct conversion of fibroblasts into motoneurons. Several protocols have been developed for differentiation of human ES cells into motoneurons and Hb9 expression appears to be specific to the motoneurons originating from the pMN domain in the developing human spinal cord (Amoroso et al., 2013; Li et al., 2008; Marklund et al., 2014). The enhancers for Hb9 used in this study were derived from the mouse genome but have been shown to be approximately 98% (Enhancer A) and 96% (Enhancer B) homologous to the human genome (Nakano et al., 2005), suggesting that the Hb9-Puro selection vector may be appropriate for human motoneuron purification. Transition to human cells will depend on successful integration and expression of the Hb9-Puro vector, specific expression of Hb9 in post-mitotic motoneurons, and successful culture of selected motoneurons.

In this study, we demonstrate that Hb9-driven puromycin resistance can be used as a simple method for purification of ES cell-derived motoneurons. The resulting population maintains the characteristics of ES cell-derived motoneurons and embryonic spinal motoneurons (Fig. 11). While PAC is a bacterial drug resistance enzyme and may not be appropriate for regenerative medicine applications in the clinical setting, puromycin selection of ES cell-derived motoneurons has many advantages for pre-clinical and in vitro studies. By producing a nearly pure population of cells, this technique can provide a uniform and consistent platform for drug screening and for the study of motoneuron disease such as ALS.

The neurofilament, MNR2/Hb9, and ChAT monoclonal antibodies developed by T.M. Jessell and S. Brenner-Morton, T.M. Jessell and J. Dodd, and P.M. Salvaterra, respectively, were obtained from the Developmental Studies Hybridoma Bank developed under the auspices of the NICHD and maintained by the University of Iowa, Department of Biology, Iowa City, IA 52242.

References

Amoroso MW, Croft GF, Williams DJ, O'Keeffe S, Carrasco MA, Davis AR, Roybon L, Oakley DH, Maniatis T, Henderson CE, Wichterle H. 2013. Accelerated high-yield generation of limb-innervating motor neurons from human stem cells. J Neurosci 33:574–586.

Anderson D, Self T, Mellor IR, Goh G, Hill SJ, Denning C. 2007. Transgenic enrichment of cardiomyocytes from human embryonic stem cells. Mol Ther 15:2027–2036.

Arber S, Han B, Mendelsohn M, Smith M, Jessell TM, Sockanathan S. 1999. Requirement for the homeobox gene Hb9 in the consolidation of motor neuron identity. Neuron 23:659–674.

Bean BP. 2007. The action potential in mammalian central neurons. Nat Rev Neurosci 8:451–465.

Bohl D, Liu S, Blanchard S, Hocquemiller M, Haase G, Heard JM. 2008. Directed evolution of motor neurons from genetically engineered neural precursors. Stem Cells 26:2564–2575.

Camu W, Henderson CE. 1992. Purification of embryonic rat motoneurons by panning on a monoclonal antibody to the low-affinity NGF receptor. J Neurosci Methods 44:59–70.

Carrascal L, Nieto-Gonzalez JL, Cameron WE, Torres B, Nunez-Abades PA. 2005. Changes during the postnatal development in physiological and anatomical characteristics of rat motoneurons studied in vitro. Brain Res Brain Res Rev 49:377–387.

Deshpande DM, Kim YS, Martinez T, Carmen J, Dike S, Shats I, Rubin LL, Drummond J, Krishnan C, Hoke A, Maragakis N, Shefner J, Rothstein JD, Kerr DA. 2006. Recovery from paralysis in adult rats using embryonic stem cells. Ann Neurol 60:32–44.

Espuny-Camacho I, Michelsen KA, Gall D, Linaro D, Hasche A, Bonnefont J, Bali C, Orduz D, Bilheu A, Herpoel A, Lambert N, Gaspard N, Peron S, Schiffmann SN, Giugliano M, Gaillard A, Vanderhaeghen P. 2013. Pyramidal neurons derived from human pluripotent stem cells integrate efficiently into mouse brain circuits in vivo. Neuron 77:440–456.

Gaspard N, Bouschet T, Herpoel A, Naeije G, van den Ameele J, Vanderhaeghen P. 2009. Generation of cortical neurons from mouse embryonic stem cells. Nat Protoc 4:1454–1463.

Gingras M, Gagnon V, Minotti S, Durham HD, Berthod F. 2007. Optimized protocols for isolation of primary motor neurons, astrocytes and microglia from embryonic mouse spinal cord. J Neurosci Methods 163:111–118.

Gruber H, Zenker W. 1973. Acetylcholinesterase: Histochemical differentiation between motor and sensory nerve fibres. Brain Res 51:207–214.

Kanaya F, Ogden L, Breidenbach WC, Tsai TM, Scheker L. 1991. Sensory and motor fiber differentiation with Karnovsky staining. J Hand Surg Am 16:851–858.

Kim JH, Auerbach JM, Rodriguez-Gomez JA, Velasco I, Gavin D, Lumelsky N, Lee SH, Nguyen J, Sanchez-Pernaute R, Bankiewicz K, McKay R. 2002. Dopamine neurons derived from embryonic stem cells function in an animal model of Parkinson's disease. Nature 418:50–56.

Kim M, Habiba A, Doherty JM, Mills JC, Mercer RW, Huettner JE. 2009. Regulation of mouse embryonic stem cell neural differentiation by retinoic acid. Dev Biol 328:456–471.

Lee SH, Lumelsky N, Studer L, Auerbach JM, McKay RD. 2000. Efficient generation of midbrain and hindbrain neurons from mouse embryonic stem cells. Nat Biotechnol 18:675–679.

Li XJ, Hu BY, Jones SA, Zhang YS, Lavaute T, Du ZW, Zhang SC. 2008. Directed differentiation of ventral spinal progenitors and motor neurons from human embryonic stem cells by small molecules. Stem Cells 26:886–893.

Mancini C, Messana E, Turco E, Brussino A, Brusco A. 2011. Gene-targeted embryonic stem cells: Real-time PCR assay for estimation of the number of neomycin selection cassettes. Biol Proced Online 13:10.

Marklund U, Alekseenko Z, Andersson E, Falci S, Westgren M, Perlmann T, Graham A, Sundstrom E, Ericson J. 2014. Detailed expression analysis of regulatory genes in the early developing human neural tube. Stem Cells Dev 23:5–15.

McCreedy DA, Rieger CR, Gottlieb DI, Sakiyama-Elbert SE. 2012. Transgenic enrichment of mouse embryonic stem cell-derived progenitor motor neurons. Stem Cell Res 8:368–378.

Miles GB, Yohn DC, Wichterle H, Jessell TM, Rafuse VF, Brownstone RM. 2004. Functional properties of motoneurons derived from mouse embryonic stem cells. J Neurosci 24:7848–7858.

Murashov AK, Pak ES, Hendricks WA, Owensby JP, Sierpinski PL, Tatko LM, Fletcher PL. 2005. Directed differentiation of embryonic stem cells into dorsal interneurons. FASEB J 19:252–254.

Nakano T, Windrem M, Zappavigna V, Goldman SA. 2005. Identification of a conserved 125 base-pair Hb9 enhancer that specifies gene expression to spinal motor neurons. Dev Biol 283:474–485.

Salero E, Hatten ME. 2007. Differentiation of ES cells into cerebellar neurons. Proc Natl Acad Sci USA 104:2997–3002.

Schnaar RI, Schaffner AE. 1981. Separation of cell types from embryonic chicken and rat spinal cord: Characterization of motoneuron-enriched fractions. J Neurosci 1:204–217.

Singh Roy N, Nakano T, Xuing L, Kang J, Nedergaard M, Goldman SA. 2005. Enhancer-specified GFP-based FACS purification of human spinal motor neurons from embryonic stem cells. Exp Neurol 196:224–234.

Takazawa T, Croft GF, Amoroso MW, Studer L, Wichterle H, Macdermott AB. 2012. Maturation of spinal motor neurons derived from human embryonic stem cells. PLoS ONE 7:e40154.

Traynelis SF, Wollmuth LP, McBain CJ, Menniti FS, Vance KM, Ogden KK, Hansen KB, Yuan H, Myers SJ, Dingledine R. 2010. Glutamate receptor ion channels: Structure, regulation, and function. Pharmacol Rev 62: 405–496.

Veyrat-Durebex C, Corcia P, Dangoumau A, Laumonnier F, Piver E, Gordon PH, Andres CR, Vourc'h P, Blasco H. 2013. Advances in cellular models to explore the pathophysiology of amyotrophic lateral sclerosis. Mol Neurobiol 49:966–983.

Wada T, Honda M, Minami I, Tooi N, Amagai Y, Nakatsuji N, Aiba K. 2009. Highly efficient differentiation and enrichment of spinal motor neurons derived from human and monkey embryonic stem cells. PLoS ONE 4: e6722.

Wichterle H, Lieberam I, Porter JA, Jessell TM. 2002. Directed differentiation of embryonic stem cells into motor neurons. Cell 110:385–397.

Wichterle H, Peljto M. 2008. Differentiation of mouse embryonic stem cells to spinal motor neurons. Curr Protoc Stem Cell Biol Chapter 1: Unit 1H 1 1-1H1.9.

Wichterle H, Peljto M, Nedelec S. 2009. Xenotransplantation of embryonic stem cell-derived motor neurons into the developing chick spinal cord. Methods Mol Biol 482:171–183.

Xian H, Gottlieb DI. 2004. Dividing Olig2-expressing progenitor cells derived from ES cells. Glia 47:88–101.

Supporting Information

Additional Supporting Information may be found in the online version of this article at the publisher's web-site.

Supplemental Table I. Analysis of Isolated Transgenic Embryonic Stem Cell Clones

Parameter	Result
# of clones isolated	24
# with puromycin resistant motoneurons	12
Minimum PAC copy number	0.242
Maximum PAC copy number	8.94
PAC copy number of selected clone	0.94

Supplemental Table II. Physiological Parameters

parameter	Sodium Current	Calcium Currents (14)
peak current	-2.25 ± 0.17 nA (77)	-453.7 ± 69.5 pA
peak V_m	-26.6 ± 0.8 mV (77)	-20.7 ± 2.5 mV
activation $V_{1/2}$	-33.6 ± 1.4 mV (13)	-26.3 ± 1.6 mV
slope	2.7 ± 0.4 mV (13)	3.5 ± 0.6 mV
inactivation $V_{1/2}$	-41.9 ± 1.4 mV (38)	N.D.
slope	7.6 ± 0.4 mV (38)	N.D.
	Potassium Currents (8)	
	transient	**sustained**
maximal conductance	13.7 ± 2.7 pS	19.2 ± 3.1 pS
activation $V_{1/2}$	-15.5 ± 5.6 mV	11.3 ± 2.5 mV
slope	12.3 ± 1.8 mV	20.6 ± 0.9 mV
inactivation $V_{1/2}$	-56.0 ± 1.8 mV	N.D.
slope	10.4 ± 0.4 mV	N.D.

Supplemental Table III. Comparison of ES-derived motoneurons identified by puromycin resistance or GFP expression driven by the Hb9 promoter

Parameter	Puromycin	GFP
peak I Na	-2.25 ± 0.17 nA (77)	-3.75 ± 0.30 nA (35)
Vm for peak I Na	-26.6 ± 0.8 mV (77)	-20 mV
capacitance	49.27 ± 1.9 pF (91)	31.3 ± 1.1 pF (71)
V rest	-60.4 ± 1.2 mV (10)	-53 ± 1 mV (71)
R input	827 ± 136 MOhm (19)	570 28 MOhm (71)
maximal AP frequency	27.8 ± 2.5 Hz (6)	18.4 ± 0.3 Hz (9)
minimal AP frequency	9.3 ± 0.6 Hz (6)	5.1 ± 0.4 Hz (13)
conductance increase (%)		
100 µM GABA	3400 ± 2100 (8)	465 ± 168 (4)
100 µM glycine	3200 ± 1500 (10)	62 ± 17 (6)
100 µM kainate	98 ± 57 (7)	
100 µM NMDA	26 ± 15 (7)	
100 µM glutamate		41 ± 17 (5)

Values for motoneurons identified by Hb9 driven GFP expression come from Miles et al. *Journal of Neuroscience* **24**:7848-58, 2004.